Der Alexander von Humboldt-Stiftung sind wir zu großem Dank verpflichtet für die großzügige Unterstützung unserer Arbeit. Herr Prof. Dr. K. UEBERREITER hat uns freundlicherweise mit Rat und Tat bei der Aufnahme der Aufschmelzkurven geholfen. Herrn Dr. K. WÜNDRICH von der Bundesanstalt für Materialprüfung sind wir für die Bestrahlung der Proben zu Dank verpflichtet.

1 N. KASAI u. M. KAKUDO, J. Polymer Sci. **A 2,** 1955 [1964].
2 R. CORNELIUSSEN u. A. PETERLIN, Makromol. Chem. **105,** 192 [1967].
3 A. PETERLIN u. F. J. BALTÁ-CALLEJA, Kolloid-Z. u. Z. Polymere **242,** 1093 [1970].
4 I. L. HAY u. A. KELLER, Kolloid-Z. u. Z. Polymere **204,** 43 [1965].
5 F. J. BALTÁ-CALLEJA, H. ČAČKOVIĆ, R. HOSEMANN u. W. WILKE, Kolloid-Z. u. Z. Polymere **206,** 118 [1965].
6 W. GLENZ, A. PETERLIN u. W. WILKE, J. Polymer Sci. **A 2, 9,** 1243 [1971].
7 H. E. BAIR, R. SALOVEY u. T. W. HINSEBY, Polymer **8,** 9 [1967].
8 R. HOSEMANN u. S. N. BAGCHI, Direct Analysis of Diffraction by Matter, North-Holland Publ. Co., Amsterdam 1962. W. WILKE u. R. HOSEMANN, Faserforsch. Textiltechn. **18,** 54 [1967].
9 F. J. BALTÁ-CALLEJA, R. HOSEMANN u. W. WILKE, Makromol. Chem. **92,** 25 [1966].
10 R. HOSEMANN, Ber. Bunsenges. Physikal. Chem. **74,** 755 [1970]. — J. LOBODA-ČAČKOVIĆ, R. HOSEMANN u. H. ČAČKOVIĆ, J. Materials Sci. **6,** 269 [1971].
11 Veröffentlichung in Vorbereitung.

Some Characteristics of Dynamical Diffraction at a Bragg Angle of about $\pi/2$ *

K. KOHRA and T. MATSUSHITA

Department of Applied Physics, Faculty of Engineering, University of Tokyo, Tokyo, Japan

(Z. Naturforsch. **27 a,** 484—487 [1972]; received 16 January 1972)

Dedicated to Prof. Dr. K. MOLIÈRE *on his 60-th Birthday*

The diffraction phenomena of X-rays in the case $\Theta_B \cong \pi/2$ are studied on the basis of dynamical theory. The angular width of diffraction for $\Theta_B = \pi/2$, $2\sqrt{|\chi_h|}$, is about 10^3 times as broad as the one for $\Theta_B \ll \pi/2$, $2|\chi_h|/\sin\Theta_B$. Similar characteristic phenomena are expected for electrons. The $\pi/2$ Bragg angle diffraction would be utilized as X-ray resonator.

In the conventional dynamical theory of X-ray and electron diffractions it is assumed that the Bragg angle, Θ_B, or the angle between the incident or diffracted beam and the crystal surface, Θ_0 or Θ_h, is not close to $\pi/2$ nor zero. On the other hand, some extreme cases such as $\Theta_B \cong 0$ and Θ_0 or $\Theta_h \cong 0$ have been studied by many workers because of their characteristic phenomena, e. g., Kikuchi Bands of lower indices [1], anomalies of diffraction at grazing angle of incidence [2], and channeling effects [3] in the case $\Theta_B \cong 0$ for electrons; Kikuchi-envelope [4] and anomalous enhancement of mirror reflection [5, 6] in the case $\Theta_h \cong 0$ for electrons; asymmetric-case diffraction [7] in the case Θ_0 or $\Theta_h \cong 0$ for X-rays. However, it seems that the case $\Theta_B \cong \pi/2$ has not been studied on the basis of the dynamical theory with the exception of a general consideration on the dispersion surface of electrons by STERN et al. [8], although precise measurements of lattice spacing for X-rays [9] under the condition of this case have sometimes been made. In this note we report some characteristics of this extreme case, mainly for X-rays, and some probable applications.

At first we consider the case of X-ray diffraction, and, for simplicity, deal with the case of two-beam approximation. According to the dynamical theory, as well known, the secular equation of the reduced wave equations is given as

$$\begin{vmatrix} \dfrac{\boldsymbol{k}_0^2 - k^2}{K^2} & \chi_{\bar{h}} \\ \chi_h & \dfrac{\boldsymbol{k}_h^2 - k^2}{K^2} \end{vmatrix} = 0 \qquad (1)$$

where

$$\boldsymbol{k}_h = \boldsymbol{k}_0 + \boldsymbol{h} \quad \text{and} \quad k = K/\sqrt{1+\chi_0}\,; \qquad (2)$$

$\boldsymbol{k}_0$ and $\boldsymbol{k}_h$ are the wave vectors of the incident and diffracted waves in the crystal, $\boldsymbol{h}$ the reciprocal lat-

Reprint requests to Prof. Dr. K. KOHRA, Department of Applied Physics, Faculty of Engineering, University of Tokyo, 113, Hongo, Bunkyo-ku, Tokyo, Japan.

* Read by K. KOHRA at the Meeting of Phys. Soc. Japan, 1 April, 1969, and by T. MATSUSHITA and K. KOHRA at the Meeting of Phys. Soc. Japan, 9 April 1971.

tice vector for the diffraction, K the wave number of the incident wave in vacuum and χ_0 and χ_{h} 4π times the Fourier components of the polarizability of the crystal.

For convenience we assume that the diffracting plane is parallel to the entrance surface. We are now concerned with the case $\Theta_{\mathrm{B}} \cong \pi/2$, in other words, $k \cong h/2$ or $\lambda \cong 2d$ from the Bragg condition. Here λ and Θ_{B} relate to the crystal corrected by the refractive index. The dispersion surface for $k = h/2 - \varepsilon$ $(\varepsilon > 0)$ is schematically drawn in Fig. 1,

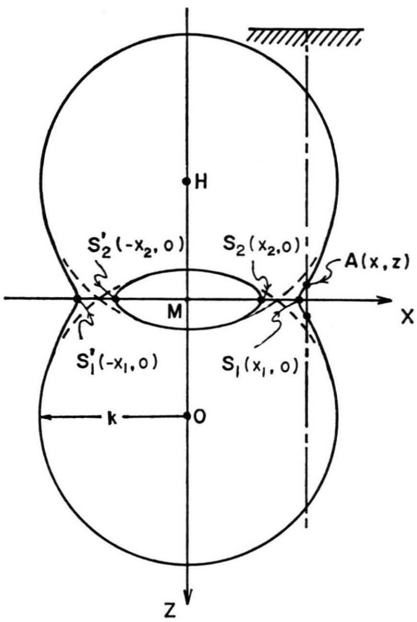

Fig. 1. A dispersion surface for $k > h/2$.

where the origin of the coordinate is taken at the middle of the reciprocal points, O and H, and x- and z-axes normal and paralel to $\overrightarrow{\mathrm{HO}}$, respectively. The wave point A, for which we have $\overrightarrow{\mathrm{AO}} = \boldsymbol{k}_0$ and $\overrightarrow{\mathrm{AH}} = \boldsymbol{k}_{\mathrm{h}}$, is represented as $A(x, z)$. With use of the relations

$$\boldsymbol{k}_0 = x\,\boldsymbol{x} + (h/2 - z)\,\boldsymbol{z} \text{ and } \boldsymbol{k}_{\mathrm{h}} = x\,\boldsymbol{x} - (h/2 + z)\,\boldsymbol{z}$$

where $\boldsymbol{x}$ and $\boldsymbol{z}$ are the unit vectors along the x- and z-axes, respectively, Eq. (1) is rewritten as

$$z^2 = \frac{x^2 - (k^2 - h^2/4)^2 - k^2 \chi_{\mathrm{h}} \chi_{\bar{\mathrm{h}}}}{2(k^2 + h^2/4 - x^2)}. \tag{3}$$

The magnitude of k or λ is classified as follows:

(i) $h/2k(=\lambda/2d) < 1 - |\chi_{\mathrm{h}}|/2$,
(ii) $1 - |\chi_{\mathrm{h}}|/2 < h/2k(=\lambda/2d) < 1 + |\chi_{\mathrm{h}}|/2$,
(iii) $h/2k(=\lambda/2d) > 1 + |\chi_{\mathrm{h}}|/2$ *.

Dispersion surfaces corresponding to (i) and (ii) near the region satisfying the Bragg condition are schematically drawn in Figure 2. In the region (ii) there are no real values of z for $x = 0$. The region (i) corresponds to the case which is considered in

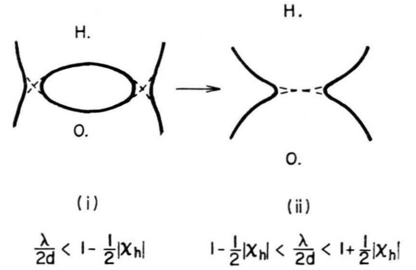

Fig. 2. Disersion surfaces near the region of selective reflection.

the conventional dynamical theory. The present study is concerned with the region (ii). The range of selective reflection, for which z is imaginary, corresponds to

$$\overline{S_1 S_2} = \sqrt{k^2 - h^2/4 + k^2|\chi_{\mathrm{h}}|} - \sqrt{k^2 - h^2/4 - k^2|\chi_{\mathrm{h}}|}$$

for (i), while

$$\overline{S_1 S_1'} = 2\sqrt{k^2 - h^2/4 + k^2|\chi_{\mathrm{h}}|} \tag{5}$$

for (ii). The variation of the range of selective reflection with wavelength or wave number is schema-

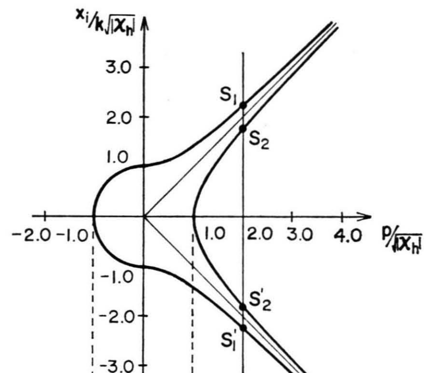

Fig. 3. Variation of range of selective reflection with wave number. $p = \mathrm{sign}\{k - h/2\}\sqrt{k^2 - h^2/4}/k$. x_i $(i = 1, 2)$ is the abscissa of S_i in Figure 1. The ranges of selective reflection are $\overline{S_1 S_2}$ and $\overline{S_1' S_2'}$ for (i), while $\overline{S_1 S_1'}$ for (ii).

tically shown in Figure 3. In case (i), and when $h/k \ll 1 - |\chi_{\mathrm{h}}|/2$ or $\Theta_{\mathrm{B}} \ll \pi/2$, we have

$$\overline{S_1 S_2} = k^2|\chi_{\mathrm{h}}|/\sqrt{k^2 - h^2/4}$$

* Here, for simplicity, $\chi_{\mathrm{h}} = \chi_{\bar{\mathrm{h}}}$ and accordingly $|\chi_{\mathrm{h}}|^2 = \chi_{\mathrm{h}} \chi_{\bar{\mathrm{h}}}$ are assumed.

and, correspondingly, the angular range of selective reflection is given by

$$\Delta\Theta = 2\,|\chi_h|/\sin 2\,\Theta_B\,. \tag{6}$$

On the other hand, in case of (ii), and when $k = h/2$ or $\Theta_B = \pi/2$, we have $\overline{S_1 S_1'} = 2\,k\sqrt{|\chi_h|}$ and, correspondingly,

$$\Delta\Theta = 2\sqrt{|\chi_h|}\,. \tag{7}$$

It is to be noted that the angular width of selective reflection in the case $\Theta_B = \pi/2$ is broader by a factor of $10^2 \sim 10^3$ than the one in the usual case where $\Theta_B \ll \pi/2$, since $|\chi_h|$ is of the order 10^{-6}. The angular widths of Si 444 diffraction for different wavelengths are compared in Table 1.

Table 1. Angular widths of Si 444 diffraction.

Wavelength (Å)	Bragg angle	Angular width of selective reflection
1.567756	90° 0′	820″
1.540562 ($CuK\alpha_1$)	79° 19′	5.3″
0.709300 ($MoK\alpha_1$)	26° 54′	0.5″

On the other hand, the extinction distance, t_0, at which the intensities of the waves in the crystal decrease to $1/e$ of those at the surface when the diffraction condition is just satisfied, is the same for the cases (i) and (ii) and is given by

$$t_0 = \sin\Theta_B / 2\,\pi\,k\,|\chi_h|\,. \tag{8}$$

As for the diffracted and transmitted intensities, calculations based on the ordinary procedure show that the expressions for case (ii) are obtained by replacing a well known parameter, say y, which indicates the deviation from the diffraction condition, by y^2 in those obtained by the ordinary theory for case (i). The calculated intensity curves of the wave diffracted from a plane parallel plate of a non-absorbing crystal are compared for the cases (i) and (ii) in Fig. 4, where the curves are given in y-scale so that the range of selective reflection is about the same although the corresponding angular range is much broader for case (ii) than for case (i).

When diffraction takes place at the Bragg angle $\pi/2$ or its vicinity, the energy of X-rays is concentrated in a shallow region of a few micron in depth under the crystal surface and also in the direction normal to the incident beam. On the other hand, in the usual Bragg-case diffraction where the Bragg angle is not close to $\pi/2$, the energy flows along the surface although it is concentrated in a shallow layer under the surface. The concentration of X-rays in the $\pi/2$ Bragg-angle diffraction would be useful for studies on some secondary effects such as secondary X-rays and electrons emitted in the process of diffraction.

It is also possible to concentrate X-ray beam on a straight line between the two diffracting crystals of $\pi/2$ Bragg angle which are placed face to face. This system could be utilized as resonator of an X-ray laser. Compared with proposals [10-12] previously made the present method would be easier in tuning because of its very broad angular range of diffraction, and more efficient because of the concentration of X-rays on a straight path instead of side paths of a polygon. A suitable reflectivity or transmissivity could be chosen by varying the crystal thickness. Unfortunately, it is rather rare for a characteristic radiation usually used to find out a proper diffracting plane in high-quality crystals. However, we can find some probable combinations of wavelength and diffracting plane, a few examples of which are shown in Table 2. With the use of some

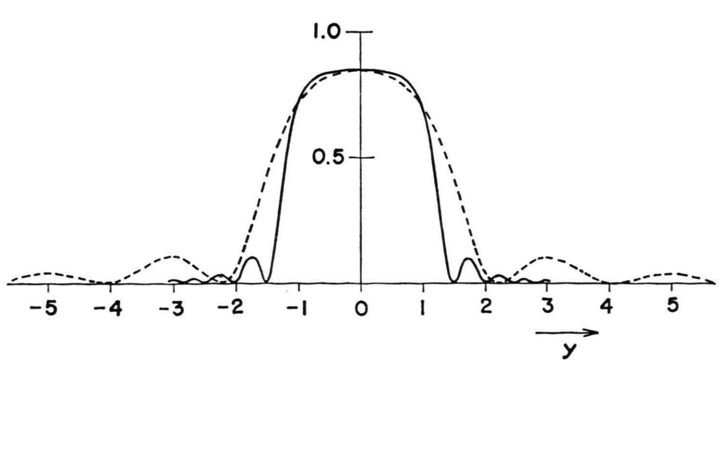

Fig. 4. Diffracted intensity from a non-absorbing crystal plate when $A = \pi\,k\,|\chi_h|\,D/\sin\Theta_B$ is $\pi/2$, where D is the crystal thickness. The solid curve is for $\pi/2$ Bragg angle diffraction and the broken one for the ordinary case where $\Theta_B \ll \pi/2$.

techniques, e. g. by changing slightly the lattice spacing thermally or mechanically, the condition for the $\pi/2$ Bragg-angle difraction could be exactly satisfied.

Table 2. Combinations of diffracting plane and characteristic X-rays for the $\pi/2$ Bragg angle (d^*: lattice spacing).

Diffracting plane	$2\,d^*$ (Å)	Characteristic X-Rays (Å)
Si 533	1.656398	1.657910 ($NiK\alpha_1$)
Si 555, 751	1.254205	1.254054 ($GeK\alpha_1$)
Ge 620	1.78910	1.788965 ($CoK\alpha_1$)
LiF 640	1.11689	1.11686 ($GeK\beta_2$)

Needless to say, it is not a problem to find out an appropriate wavelength in the continuous X-rays, but the intensity would come into question. In the diffraction at Bragg angle $\cong \pi/2$ it is technically impossible or very difficult to measure the diffracted intensity, but it is easy to measure the transmitted beam and its dependence on crystal thickness.

In the case of electron diffraction it is not a problem to find out an appropriate wavelength satisfying the condition $\Theta_B = \pi/2$ for a diffracting plane. However, it is clear that the two-beam approximation is no longer valid, but some essential features common to those in X-ray diffraction would be found. Measurements would be also easier in electron diffraction because the incident and diffracted beams can be curved in opposite directions with a magnetic field. A detailed study will be reported in the near future.

[1] M. VON LAUE, Materiewellen und ihre Interferenzen, Akad. Verl. Leipzig 1944, p. 343; P. B. HIRSCH et al., Electron Microscopy of Thin Crystals, Butterworths, London 1965, p. 447.

[2] K. KOHRA and K. SHINOHARA, J. Phys. Soc. Japan **4**, 155, 166 [1949].

[3] A. HOWIE, Modern Diffraction and Imaging Techniques in Material Science, edited by S. AMERINCKX et al., North-Holland Publ. Co., Amsterdam 1970, p. 312; V. E. COSSLETT, ibid., p. 354.

[4] M. VON LAUE, Materiewellen und ihre Interferenzen, Akad. Verl. Leipzig 1944, p. 349.

[5] S. MIYAKE, K. KOHRA, and M. TAKAGI, Acta Cryst. **7**, 393 [1954].

[6] K. KOHRA, S. NAKANO, and K. MOLIÈRE, J. Phys. Soc. Japan, Suppl. II, 82 [1962].

[7] S. KISHINO and K. KOHRA, Japan. J. Appl. Phys. **10**, 551 [1971].

[8] R. M. STERN, J. J. PERRY, and D. S. BOUDREUX, Rev. Mod. Phys. **41**, 275 [1969].

[9] B. SYKORA and H. PEISEL, Z. Angew. Physik **30**, 320 [1970].

[10] W. L. BOND, M. A. DUGAY, and P. M. RENTZEPIS, Appl. Phys. Letters **10**, 216 [1967].

[11] R. D. DESLATTES, Appl. Phys. Letters **12**, 133 [1968].

[12] R. M. CETERILL, Appl. Phys. Letters **12**, 403 [1968].